Entanglement of Two, Three or Four Plasmonically Coupled Quantum Dots

Matthew Otten,[1,2] Raman A. Shah,[3] Norbert F. Scherer,[3]
Misun Min,[2] Matthew Pelton,[4] and Stephen K. Gray[5]

[1]*Department of Physics, Cornell University, Ithaca, NY 14853*

[2]*Mathematics and Computer Science Division,*
Argonne National Laboratory, Argonne, IL 60439

[3]*Department of Chemistry and The James Franck Institute,*
The University of Chicago, Chicago, IL 60637

[4]*Department of Physics, University of Maryland,*
Baltimore County, Baltimore, MD 21250

[5]*Center for Nanoscale Materials, Argonne National Laboratory, Argonne, IL 60439*

(Dated: December 15, 2015)

Abstract

We model the quantum dynamics of two, three, or four quantum dots in proximity to a plasmonic system such as a metal nanoparticle or an array of metal nanoparticles. For all systems, an initial state with only one quantum dot in its excited state evolves spontaneously into a state with entanglement between all pairs of QDs. The entanglement arises from the couplings of the QDs to the dissipiative, plasmonic environment. Moreover, we predict that similarly entangled states can be generated in systems with appropriate geometries, starting in their ground states, by exciting the entire system with a single, ultrafast laser pulse. By using a series of repeated pulses, the system can also be prepared in an entangled state at an arbitrary time.

PACS numbers: 03.67.Bg,42.50.Dv,42.50.Md,42.50.Pg,73.20.Mf,78.67.Bf

I. INTRODUCTION

Plasmonic nanostructures provide the potential for extremely strong light-matter interactions because of their ability to concentrate optical fields to nanometer-scale dimensions.[1] Such strong interactions could enable the manipulation of quantum states in materials that interact with the confined fields.[2–4] However, plasmon resonances are necessarily associated with strong dissipation, raising the question of whether quantum effects are compatible with such rapid loss of energy and coherence.

On the other hand, it has been realized that controlled interactions between quantum objects and a dissipative environment can lead to the production of stable entangled states .[5–7] Several theoretical studies applied this concept of dissipation-induced entanglement to problems of QDs interacting with plasmonic systems .[8–13] These studies show that effective interactions between pairs of two-level quantum dots (QDs), mediated by dissipative plasmon resonances in metal nanoparticles or waveguides,[14] can produce entanglement between QDs, analogous to previous proposals to entangle interacting atoms through common coupling to a lossy cavity.[15] The QDs' entanglement arises spontaneously due to common coupling to the plasmonic nanostructures, without requiring postselective measurements or "engineering" of the dissipative environment. Since entanglement is a uniquely quantum property that is at the heart of quantum information and computation, this illustrates in principle the potential for true "quantum plasmonics" .[16] Such QD-plasmonic systems are also of relevance because they represent nanoscale structures that do not require atom traps or cryogenic temperatures to operate and can be integrated with other nanophotonic components.

Despite their potential for displaying quantum plasmonics effects, previous predictions of plasmon-induced entanglement in QDs have been limited to systems of only two QDs, and one of the QDs was required to be initially prepared in its excited state. For systems of two QDs, this can, in principle, be done using single-photon pulses,[17] but scaling these schemes up to larger numbers of QDs would require the ability to individually access and control the state of each QD.

In this paper, we propose a system where control over the interaction between objects to be entangled (QDs) and the dissipative environment (plasmonic system) is determined by the nanoscale geometry of the system, and the only external input required is a single, ultrafast laser pulse. Moreover, we show that the method can be scaled to multiple QDs,

and thus has the potential to serve as a key resource for quantum information processing at the nanoscale.[18,19]

II. THEORETICAL METHODS

Our treatment, detailed in the Supporting Materials, generalizes our work on one QD interacting with a plasmonic system.[20] The underlying system basis states are $|q_{N_D}, ..., q_1\rangle\,|s\rangle$, where $q_i \in \{\,0, 1\,\}$ indexes the exciton in QD i; i ranges from 1 to N_D (the number of QDs) and s indexes plasmon energy levels. Lowering and raising operator pairs for the QDs and plasmon are $(\hat{\sigma}_i, \hat{\sigma}_i^\dagger)$, and $(\hat{b}, \hat{b}^\dagger)$, respectively. The dipole operators are $\hat{\mu}_i = d_i(\hat{\sigma}_i + \hat{\sigma}_i^\dagger)$, and $\hat{\mu}_s = d_s(\hat{b} + \hat{b}^\dagger)$, where d_i, and d_s denote transition dipole moments of the QDs and plasmon, respectively. The density matrix, $\hat{\rho}(t)$, satisfies:

$$\frac{\mathrm{d}\hat{\rho}}{\mathrm{d}t} = -\frac{i}{\hbar}[\hat{H}, \hat{\rho}] + L(\hat{\rho}), \tag{1}$$

in which $\hat{H}$ is the Hamiltonian for the driven coupled system and $L(\hat{\rho})$ is a Lindblad superoperator providing dephasing and dissipation. More explicitly,

$$\hat{H} = \sum_i \hat{H}_i + \hat{H}_s + \hat{H}_d + \sum_i \hat{H}_{s,i}, \tag{2}$$

where $\hat{H}_i = \hbar\omega_i\hat{\sigma}_i^\dagger\hat{\sigma}_i$ are uncoupled exciton Hamiltonian operators, $\hat{H}_s = \hbar\omega_s\hat{b}^\dagger\hat{b}$ is the uncoupled plasmon Hamiltonian, and $\hat{H}_d = -E(t)\hat{\mu}$ is coupling to an applied electric field, $E(t)$. Each QD couples with the plasmon via $\hat{H}_{s,i} = -\hbar g_i(\hat{\sigma}_i^\dagger\hat{b} + \hat{\sigma}_i\hat{b}^\dagger)$. We assume that the distance between QDs is large compared to the separation between QDs and neighboring metal nanoparticles, so that direct through-space coupling among QDs can be neglected. We neglect retardation, which means that our treatment is limited to systems with dimensions small compared to the optical wavelengths. The Supporting Materials discuss the level structure of $\hat{H} - \hat{H}_d$, which provides additional insight into the nature of the problem.

We employ an extension of $L(\hat{\rho})$ that was previously used,[20] parameterized by QD population (or spontaneous emission) and environmental dephasing decay constants, γ_{pi} and γ_{di}, and plasmon decay constant γ_s. We consider time scales on the order of the inverse of these decay rates, so that there are no correlated fluctuations in the QD states, and the use of the Lindblad formalism is justified. Although environmental dephasing is explicitly included for the QDs, it is not necessary to do so for the plasmon because the dephasing

that arises from its decay, and that is encoded in the corresponding term in $L(\hat{\rho})$, is much larger in magnitude. As in Ref. 20, the rotating wave approximation is applied. We use an efficient solver, based on sparse matrix-matrix multiplication algorithms along with both Runge-Kutta and exponential time integration schemes.[21,22]

The base parameter choices for the model outlined above are similar to those originally used in our single plasmonic-QD system study [20] and correspond to a gold nanoparticle system interacting with QDs in a polymer matrix. Specifically, for all i, $\hbar\omega_i = \hbar\omega_s = 2.05$ eV; $\mu_i = 13$ D, $\mu_s = 4000$ D; $\hbar\gamma_{pi} = 190$ neV, $\hbar\gamma_{di} = 2$ meV, $\hbar\gamma_s = 0.15$ eV. We assume the system is embedded in a dielectric medium of $\epsilon_{med} = 2.25$, typical of a polymer.

Electrodynamic simulations give a realistic estimate for the plasmon-QD coupling factor of $\hbar g_i \approx 10$ meV for a system of two ellipsoidal gold nanoparticles, each of length 30 nm and width 20 nm, and with a 6 nm gap between them and a QD centered in the gap.[20] Larger coupling factors could be obtained for silver nanoparticles as compared to gold,[23] for particles with larger aspect ratios or different shapes, or for smaller gaps. While such systems will exhibit different resonance frequency, linewidth, and dipole moments of the plasmon resonances, we keep those and all other parameters constant in the present calculations in order to isolate the effect of changing only the coupling constants. Calculations have been performed for coupling constants $\hbar g_i$ from 5 meV to 45 meV.

III. RESULTS

A. Entanglement in the dark

We begin by exploring a situation similar in spirit to that reported in Refs.[8,10]: one of the quantum dots (labeled "QD1") is initially in its excited state, all others are initially in their ground states, and there is no applied electromagnetic field. Unlike the previous results, however, we also consider systems with more than two QDs coupled to the plasmonic system. We quantify the degree of entanglement as a function of time using Wootters' concurrence [24] (see also Supporting Materials). Results are presented in Figs. 1(b)− (d). For the two-QD case, as previously reported,[8–10] the concurrence reaches a value of 0.45 as the system evolves. The emergence of entanglement can be understood by considering the symmetric and antisymmetric QD states,

$$|S\rangle = \frac{1}{\sqrt{2}}(|q_2 = 1, q_1 = 0\rangle + |q_2 = 0, q_1 = 1\rangle) \tag{3}$$

and

$$|A\rangle = \frac{1}{\sqrt{2}}(|q_2 = 1, q_1 = 0\rangle - |q_2 = 0, q_1 = 1\rangle) \ , \tag{4}$$

and their associated expectation values, or populations, $P_S(t)$ and $P_A(t)$, also displayed as a function of time in Fig. 1(b). The initial state, with only QD1 excited, corresponds to $P_S = P_A = 0.5$. The symmetric state, analogous to a bright singlet state, decays more rapidly than the antisymmetric state,[9] analogous to a dark triplet state. After a certain time, the population of the antisymmetric state is much larger than the population of the symmetric state, and the entanglement reaches a maximum. The results shown in Fig. 1 correspond to $\hbar g_i = 30$ meV. However, we find that entanglement, with a maximum concurrence of 0.2, can occur even for $\hbar g_i = 10$ meV (Supporting Materials). In practice the QDs may not have exactly the same energy, which could diminish the entanglement effects. However, the Supporting Materials also show that, for QDs with transition energies varying within the 2 meV dephasing width, the entanglement effects remain.

In the cases of three and four QDs, bipartite concurrence can occur between QDs that are *not* initially excited, i.e., the concurrence between QD2 and QD3, denoted 2:3, in the three-QD case (Fig. 1 (c)) and the 4:3, 4:2, 3:2 concurrences of the four-QD case (Fig. 1 (d)). Both the three-QD and four-QD cases show degeneracies in the bipartite concurrence, as the system is completely symmetric except for the one initially excited QD. All bipartite concurrences that include the initially excited QD (QD1) have a much larger peak than do the bipartite concurrences that exclude the initially excited QD.

B. Entanglement with optical pulses

So far, we have imagined that exactly one of the QDs could somehow be initially prepared in its excited state, and allowed the system to evolve from that initial state in order to generate entanglement. A more experimentally relevant situation would involve the entire plasmon-QD system starting in its ground state and being exposed to a short laser pulse. To simulate this situation, we take $E(t) = G(t)E_0\cos(\omega_0 t)$. The carrier frequency, ω_0, is taken to be on resonance with the QD transitions and the plasmon resonance: $\hbar\omega_0 = 2.05$ eV. The pulse envelope function, $G(t)$ is taken to be a Gaussian function with full-width

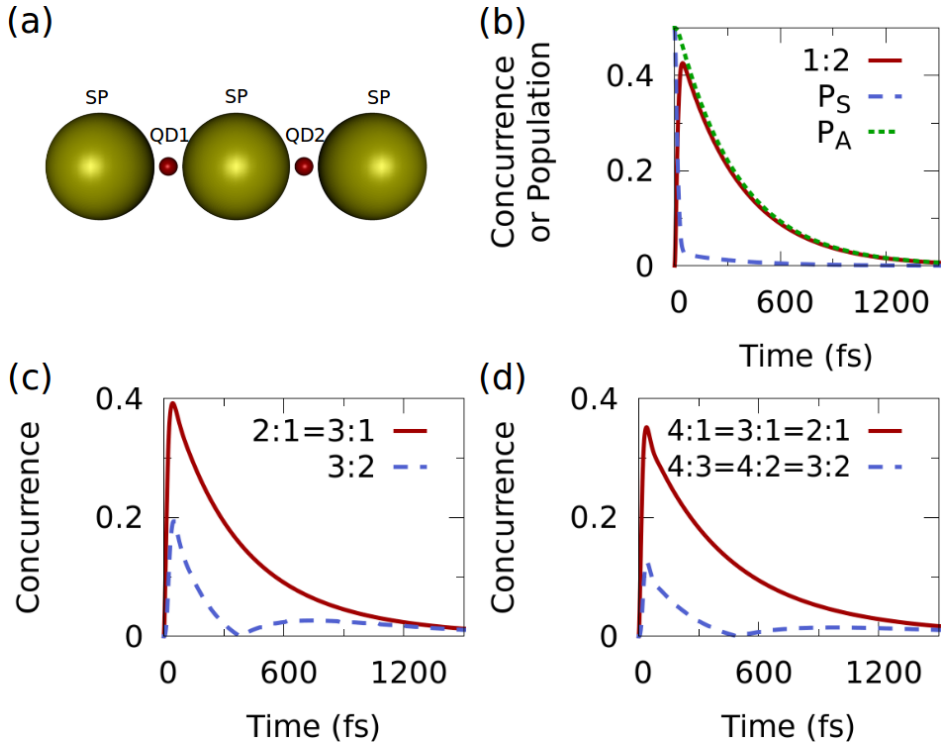

FIG. 1: (a) Diagram of a plasmonic-two-QD system composed of three metal nanoparticles (the plasmonic system, labeled 'SP') with QDs (labeled 'QD1' and 'QD2') in the interparticle gaps. Bipartite concurrence of two (b), three (c), and four (d) QD systems where one of the QDs (QD1) is initially excited, with $\hbar g_i = 30$ meV in all cases. i:j refers to the concurrence between QDi and QDj. Part (b) also shows the population of the symmetric state $|S\rangle$, P_S, and of the antisymmetric state $|A\rangle$, P_A.

at half-maximum of 20 fs, and E_0 is adjusted to achieve the desired fluence. Figure 2(a) displays the maximum concurrence that results in this case, as a function of pulse fluence (i.e., time integral of $\sqrt{\epsilon}_{med} c\epsilon_0 E^2(t)$) and plasmon-QD coupling constant for one of the QDs ($g_1 = g_2 + \Delta g$) relative to the other ($\hbar g_1 = 30$ meV). Significant parameter regions exist where the concurrence is comparable to that obtained in the dark case of Fig. 1. We should note that laser fluences up to 1000 nJ/cm^2 are both experimentally accessible and reasonable in the sense that they should not lead to sample degradation.

High concurrence occurs only when there is an asymmetry in the couplings of the QDs to the plasmonic system. This asymmetry could be achieved in practice by fabricating a system where the two QDs are at different distances from the metal nanoparticles. The asymmetry

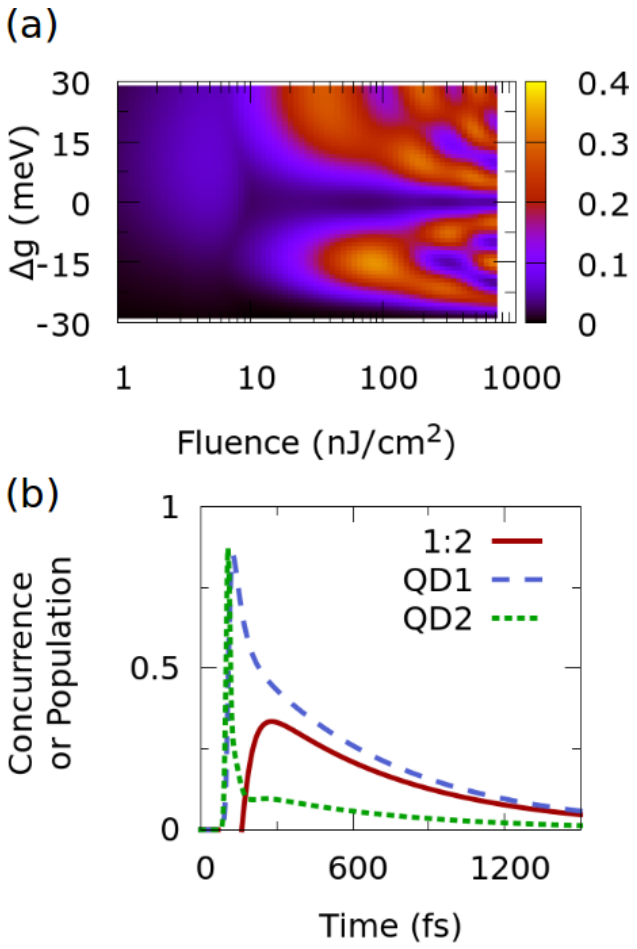

FIG. 2: Maximum concurrence when a plasmon-two-QD system initially in its ground state is exposed to a 20-fs laser pulse. (a) Concurrence as a function of laser-pulse fluence and plasmon-QD coupling coefficient for one of the QDs ($g_1 = g_2 + \Delta g$) relative to the other ($\hbar g_2 = 30$ meV). (b) Concurrence as a function of time, for coupling coefficients $\hbar g_1 = 15$ meV ($\Delta g = -15$ meV) and $\hbar g_2 = 30$ meV, and laser-pulse fluence 81 nJ/cm^2, that produce the largest concurrence. The populations of QD1 and QD2 are also plotted.

can allow one QD to be significantly more excited than the other QD by the end of the laser pulse. As a result the laser pulse then creates a QD state similar to the $|q_2 = 0, q_1 = 1\rangle$ state that was the starting point of the dark case that, as we have seen, led to a rise in concurrence. The largest concurrence for the pulsed two-QD system, ≈ 0.35, is obtained for $\hbar g_1 = 15$ meV and $\hbar g_2 = 30$ meV. The dynamics of the concurrence and QD populations for this case are shown in Fig. 2(b). One might expect that this combination of coupling coefficients would lead to larger initial population for QD2, since it is more strongly coupled

to the plasmonic system. However, the population of QD2 spikes and decays rapidly as the incident laser pulse passes through the system, while the population of QD1 rises and decays more slowly. The result is that there is eventually larger population for QD1 than QD2. This somewhat counterintuitive result, which appears to be quite general, is a consequence of the Purcell effect[20]: while the QD with the larger coupling coefficient experiences a larger local field, leading to a fast initial rise in its excited-state population, its emission rate is also increased (to $\gamma_{pi} + 4g_i^2/\gamma_s \approx 4g_i^2/\gamma_s$), leading to rapid depopulation. The QD with the smaller coupling coefficient undergoes a delayed but more sustained partial Rabi oscillation, leading to its larger initial population.

An extensive optimization such as the one we carried out for the plasmon-two-QD system is computationally challenging for larger systems. We therefore selectively examine portions of the parameter space in the three-QD case. Figure 3 depicts promising results. They are similar in spirit to the optimal two-QD result, with only one QD having a coupling different from that of the other two: $\hbar g_1 = 30$ meV, and $\hbar g_2 = \hbar g_3 = 35$ meV. Fig. 3 depicts the time evolution of the populations of the three QDs and of the bipartite concurrences. Having one QD less strongly coupled to the plasmonic system than the others allows the populations to grow and decay at different rates, so that an initial state is created with larger population in the excited state of QD1 than of QD2 or QD3. Oscillations are seen in the population of QD1 over the duration of the laser pulse, and rapid decay of the populations of QD2 and QD3 are seen due to their larger Purcell factors. Significant but smaller concurrences are found in other pulsed two-QD and three-QD systems with much smaller coupling constants, g_i, and somewhat larger fluences (Supporting Materials). Initial studies of analagous pulsed four-QD systems also indicate that such systems can be driven into entangled states, although to a degree lesser, for comparable parameters, than the two-QD and three-QD cases. In general, a more thorough investigation of the parameter space, varying other parameters such as the dephasing and decay rates, could lead to larger concurrences.

In all cases, large concurrence is achieved for only a brief period after the laser pulse has excited the system, before the population of the entangled state decays. However, entanglement can be restored to the system by applying a repeated series of pulses, as shown for a plasmon-three-QD system in Figure 4. Each incoming pulse initially destroys the entanglement and reduces concurrence to zero, because both $|A\rangle$ and $|S\rangle$ are excited. However, $|S\rangle$ decays quickly, and concurrence rapidly grows back to its peak value. For

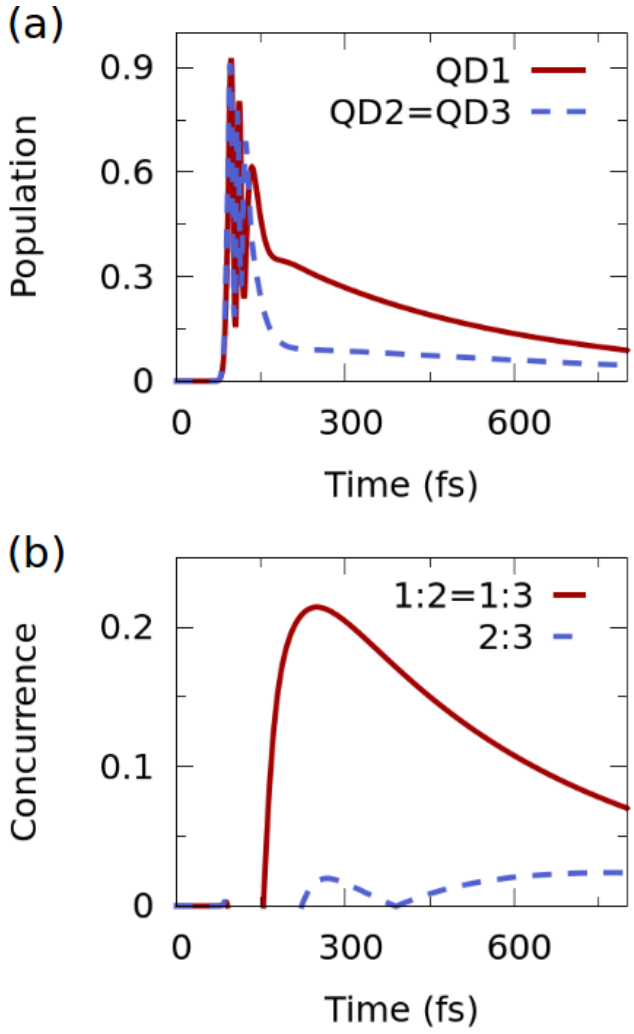

FIG. 3: Results for a plasmon-three-QD system with laser-pulse fluence of 500 nJ/cm^2, and coupling coefficients $\hbar g_1 = 30$ meV and $\hbar g_2 = \hbar g_3 = 35$ meV. (a) Excited-state populations for the three QDs. (b) Bipartite concurrences.

the concurrence between the pairs of inequivalent QDs, this peak value is somewhat smaller than the maximum value reached for a single pulse, but the peak concurrence between the two equivalent QDs is much larger than the single-pulse case. Continuous-wave excitation of the system could not induce a high degree of entanglement, as it would continually excite both the $|A\rangle$ and $|S\rangle$ states; to be entangled, the population of $|A\rangle$ needs to be large while the population of $|S\rangle$ is small.

Fabricating coupled plasmon-QD systems is a significant challenge. Our scheme requires the ability to assemble metal nanoparticles and QDs with nanometer-scale control

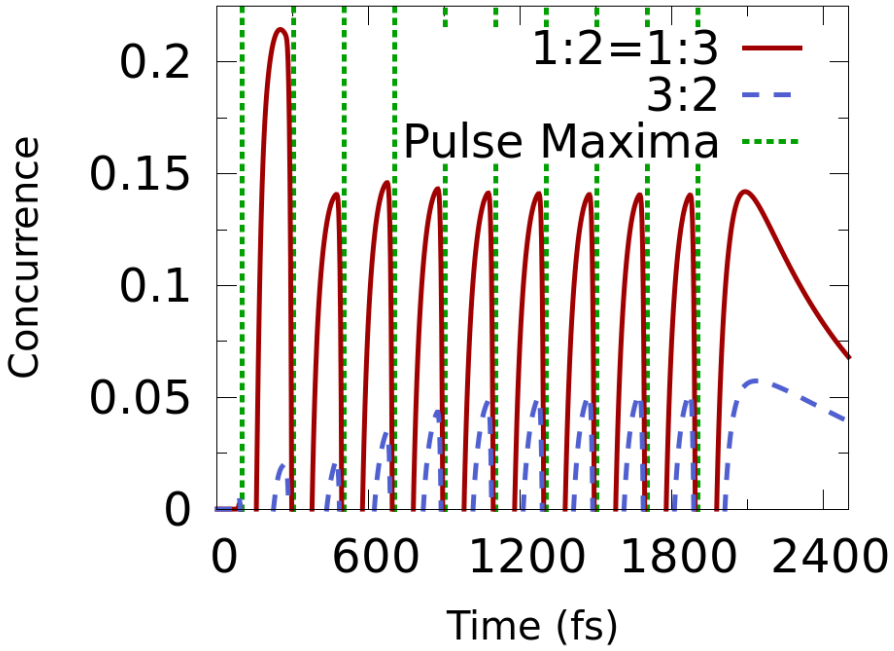

FIG. 4: Concurrences for a plasmon-three-QD system with a repeating 500 nJ/cm^2 pulse. Coupling coefficients are $\hbar g_1 = 30$ meV, $\hbar g_2 = \hbar g_3 = 35$ meV. The dotted vertical lines represent the times associated with the maxima of the pulses.

over each interparticle separation. Nonetheless, rapid improvements in nanofabrication [25] and chemically-driven nanoparticle assembly[26–29] may make it feasible in the near future. DNA self-assembly methods have recently been used, for example, to fabricate colloidal gold nanoparticles with numerous QDs surounding them,[30] and strong plasmon-emitter coupling has been experimentally demonstrated in other systems .[31]

Once a system is fabricated, there is the challenge of demonstrating entanglement. It has recently been proposed that nanoparticle plasmons could be entangled by excitation with entangled photons, and the plasmonic entanglement read out through the characteristics of the radiated far field.[32] It may be possible to use a similar scheme in our case: plasmons would be entangled through their coupling to entangled QDs, serving as a interface between the QD states and the radiated field.

IV. CONCLUDING REMARKS

In summary, we propose a scheme involving exposure to a single or repeated optical pulses, that makes it possible to create and maintain entanglement between all pairs of QDs when two, three, or four closely spaced QDs are coupled to a common plasmonic nanostructure. This contrasts with previous schemes based on plasmonic waveguides, which can entangle spatially separated dots, but which are limited to two QDs. Moreover, in our scheme, the entire system begins in its ground state and is excited by a common laser pulse or series of pulses. Tuning the degree of coupling between each QD and the plasmonic nanostructure enables generation of an excited state that evolves spontaneously, driven by dissipation of the plasmons, towards an entangled state. Entanglement is achieved without the need for the QDs to be individually addressable, and without the need for controlled quantum gates.

There are a number of considerations for achieving good concurrences. First, in general, it appears that larger magnitude QD-plasmon couplings, g_i are advantageous; here, we have restricted consideration to coupling strengths that may be achievable in practice. As noted above, engineering a system with one QD more weakly coupled to the plasmon than the others can be effective, i.e. if that QD is labeled "1" then $g_1 < g_2$, g_3, etc. For the concurrences to be maintained for appreciable lengths of time beyond the pulse, the dephasing rates should be small in comparison to the Purcell decay rates, $\gamma_{di} < 4g_i^2/\gamma_s$. Future work will involve more extensive parameter searches to discover optimal conditions than those currently found for the cases with three and more QDs coupled to a plasmonic system, as well as consideration of more sophisticated pulse shapes and sequences. Finally, we should note that the present paper focused on achieving bipartite concurrences among systems with two and more QDs. Future work will be devoted to exploration of the possibility of generating maximally entangled multi-qubit states, including what are termed GHZ and W states for three qubits.[19,33]

Acknowledgments

This work was performed, in part, at the Center for Nanoscale Materials, a U.S. Department of Energy, Office of Science, Office of Basic Energy Sciences User Facility under Contract No. DE-AC02-06CH11357. NFS thanks the Department of Defense for a National

Security Science and Engineering Faculty Fellowship.

---

[1] M. Pelton and G. Bryant, *Introduction to Metal-Nanoparticle Plasmonics* (Wiley, 2013).

[2] Z. R. Lin et al., Phys. Rev. B **82**, 24101 (2010).

[3] G. Y. Chen et al., Phys. Rev. B **84**, 045310 (2011).

[4] D. E. Chang et al., Nat. Photonics **8**, 685 (2014).

[5] J. F. Poyatos et al., Phys. Rev. Lett. **77**, 4728 (1996).

[6] Y. Lin et al., Nature **504**, 415 (2013).

[7] H. Krauter et al., Phys. Rev. Lett. **107**, 080503 (2011).

[8] A. Gonzalez-Tudela, D. Martin-Cano, E. Moreno, L. Martin-Moreno, C. Tejedor, and F. J. Garcia-Vidal, Phys. Rev. Lett. **106**, 020501 (2011).

[9] D. Martin-Cano, A. Gonzalez-Tudela, L. Martin-Moreno, F. J. Garcia-Vidal, C. Tejedor, and E. Moreno, Phys. Rev. B **84**, 235306 (2011).

[10] Y. He and K.-D. Zhu, Nanoscale Res. Lett. **7**, 95 (2012).

[11] Y. He and K.-D. Zhu, Quant. Info. Comp. **13**, 0324 (2013).

[12] C. Gonzalez-Ballestero et al., New J. Phys. **15**, 073015 (2013).

[13] C. Lee, New J. Phys. **15**, 083017 (2013).

[14] R. D. Artuso and G. W. Bryant, Phys. Rev. B **87**, 125423 (2013).

[15] S. Nicolosi et al., Phys. Rev. A **70**, 022511 (2004).

[16] M. S. Tame et al., Nature Physics **9**, 329 (2013).

[17] C. Gonzalez-Ballestero et al., Phys. Rev. A **89**, 042328 (2014).

[18] M. A. Nielsen and I. L. Chuang, *Quantum Computation and Quantum Information* (Cambridge University Press, Cambridge, 2000).

[19] R. Horodecki, P. Horodecki, M. Horodecki, and K. Horodecki, Rev. Mod. Phys. **81**, 865 (2009).

[20] R. A. Shah, N. F. Scherer, M. Pelton, and S. K. Gray, Phys. Rev. B **88**, 075411 (2013).

[21] M. Min and P. Fischer, J. Sci. Compt. **57**, 582 (2013).

[22] K. Uga, M. Min, T. Lee, and P. Fischer, Computers & Mathematics with Applications **65**, 239 (2013).

[23] X. Wu, S. K. Gray, and M. Pelton, Opt. Express **18**, 23633 (2010).

[24] W. K. Wootters, Phys. Rev. Lett. **80**, 2245 (1998).

[25] X. Chen et al., Nat. Comm. **4**, 2361 (2013).

[26] P. Kuhler et al., Nano Lett. **14**, 2914 (2014).

[27] V. V. Thacker et al., Nat. Comm. **5**, 3448 (2014).

[28] M. Geiselmann et al., Nano Lett. **14**, 1520 (2014).

[29] D. Nepal et al., ACS Nano **7**, 9064 (2013).

[30] D. Sun et al., ACS Nano **9**, 5657 (2015).

[31] G. M. Akselrod et al., Nature Photonics **8**, 835 (2014).

[32] N. Thakkar, C. Cherqui, and D. J. Masiello, ACS Photonics **2**, 157 (2015).

[33] W. Dur, G. Vidal, and J. I. Cirac, Phys. Rev. A **62**, 062314 (2000).